

Broadband channel capacities

Vittorio Giovannetti¹, Seth Lloyd^{1,2}, Lorenzo Maccone¹, and Peter W. Shor³

¹*Massachusetts Institute of Technology – Research Laboratory of Electronics
50 Vassar st., Cambridge, MA 02139, USA*

²*Massachusetts Institute of Technology – Department of Mechanical Engineering
77 Massachusetts Ave., Cambridge, MA 02139, USA*

³*AT&T Labs - Research 180 Park Ave, Florham Park, NJ 07932, USA*

(Dated: July 14, 2003)

We study the communication capacities of bosonic broadband channels in the presence of different sources of noise. In particular we analyze lossy channels in presence of white noise and thermal bath. In this context, we provide a numerical solution for the entanglement assisted capacity and upper and lower bounds for the classical and quantum capacities.

PACS numbers: 03.65.-w,03.65.Ud,03.67.-a

The study of the broadband bosonic communication channel has been one of the first applications of quantum communication theory [1, 2]. The basic result of this effort has been the determination of the ultimate limits posed by quantum mechanics to the rate at which classical information can be reliably transmitted through the channel in the noiseless case. In this context, the classical capacity C was shown to be proportional to the square root of the input power. Here we generalize these results by extending the analysis to noisy configurations and to other channel capacities such as the quantum capacity Q (the amount of quantum information that can be reliably sent through the channel) or the entanglement assisted capacity C_E (the amount of classical information that can be reliably sent through the channel in the presence of an infinite amount of prior entanglement between sender and receiver). In particular, we study various types of noise: loss (where there is a probability $1 - \eta$ that a photon is lost in the transmission line), loss with white noise or thermal reservoir coupling, and a “dephasing” channel (in which the average number of photons is preserved, but some phase correlations are lost in the transmission). In this context we determine the value of C_E as a function of the input power and show that the square root dependence applies also to most of these channels. For the other capacities we provide some bounds that establish the same dependence. A sketch of the results obtained is summarized in table I: even though implicit equations for all the capacities (or their lower bounds) have been obtained, in most of the cases numerical methods have been employed to derive their values as a function of the channel parameters.

We start by introducing the model of the channel and of its noise sources in Sec. I. We introduce capacities C_E , C and Q and the Lagrange procedure that is used to evaluate them for the broadband channel in Sec. II. The remaining sections are devoted to the analysis of the lossy channel (Sec. III), the white noise channel (Sec. IV), the thermal noise channel (Sec. V) and the dephasing channel (Sec. VI).

	C_E	C (lower bound)	Q (lower bound)
Loss	<i>numeric</i>	<i>analytic</i>	<i>numeric</i>
White noise	<i>numeric</i>	<i>analytic</i>	<i>numeric</i>
Thermal reservoir	<i>numeric</i>	<i>analytic</i>	<i>numeric</i>
Dephasing channel	<i>numeric</i>	<i>numeric</i>	<i>numeric</i>

TABLE I: Capacities calculated in the paper for different noise models.

I. GAUSSIAN BOSONIC CHANNEL

The prototype of a high capacity communication channel is an optical fiber, where time or frequency multiplexing (or hybrid strategies) are used to send information. From a fundamental point of view, such a communication line is described as a broadband bosonic channel [2]. In the present paper we analyze the performance of this channel in the realistic scenario of non-perfect transmissivity, i.e. the possibility that photons can be lost during the communication or that they can be replaced by photons coming from external noise sources. The analysis is complicated by the fact that, for some capacities, it is not known whether the additivity property holds, i.e. whether entangling successive uses of a noisy channel may increase its transmission rate [3].

Without loss of generality, we will assume that for each frequency in the channel only one polarization is used to transmit information, i.e. no frequency degeneracy is present. The quantum description of this channel is obtained by coupling each mode to a noise reservoir with beam splitters that have transmissivity equal to the quantum efficiency η_j of the j th mode, i.e.

$$a'_j = \sqrt{\eta_j} a_j + \sqrt{1 - \eta_j} b_j, \quad (1)$$

where a_j , a'_j and b_j are the annihilation operators of the input, output and noise modes respectively. The loss map \mathcal{N}_j for the j th mode arises by tracing away the noise mode b_j and the global loss map \mathcal{N} is the tensor product $\bigotimes_i \mathcal{N}_i$. Notice that for $\eta_j = 1$ the noise reservoir is

decoupled from the transmission line: this describes a noiseless channel where $\mathcal{N} = \mathbb{1}$. Different types of noise can be described depending on the initial state of the reservoir modes b_j . We will analyze the case in which the reservoir is in a separable Gaussian state of the form $\rho^{(b)} = \otimes_i \rho_i^{(b)}$ with

$$\rho_j^{(b)} = \frac{\hbar}{2\pi} \int dz \exp \left[-i z \cdot \begin{pmatrix} \Delta q_j \\ \Delta p_j \end{pmatrix} - \frac{z \cdot B_j \cdot z^T}{2} \right], \quad (2)$$

where z is a real bidimensional line vector, $\Delta q_j = q_j - \langle q_j \rangle$, $\Delta p_j = p_j - \langle p_j \rangle$, with q_j and p_j the quadratures $q_j = \sqrt{\hbar/2} (b_j^\dagger + b_j)$ and $p_j = i\sqrt{\hbar/2} (b_j^\dagger - b_j)$. For the situations in which we are interested, $\langle q_j \rangle = \langle p_j \rangle = 0$ and the correlation matrix B_j in Eq. (2) has the form

$$B_j = \hbar \begin{bmatrix} \bar{N}_j + 1/2 & 0 \\ 0 & \bar{N}_j + 1/2 \end{bmatrix}, \quad (3)$$

where \bar{N}_j is the average number of photons in the noise mode b_j . With this choice of $\rho^{(b)}$, the CP-map \mathcal{N} describes a Gaussian channel, i.e. it transforms Gaussian input states (in the modes a_j) into Gaussian output states (in a'_j).

Four different noise models will be analyzed in detail in this paper. The simplest one is a purely lossy channel in which the photons in the j th mode have a probability $1 - \eta_j$ to be lost during transmission. It is described by taking $\bar{N}_j = 0$ for all j , i.e. by taking $\rho^{(b)}$ in the vacuum. For optical communications this is the most interesting situation, since thermal photons are negligible at room temperatures. Another interesting case is given by choosing $\bar{N}_j = \bar{N}$ for all j , which describes an added white noise to the transmission. On the other hand, by choosing

$$\bar{N}_j = \frac{1}{e^{\hbar\omega_j/(KT)} - 1}, \quad (4)$$

(with ω_j the j th mode frequency) we can describe the effect of coupling the communication line to a thermal reservoir at temperature T . Of course, in the limits $\bar{N} \rightarrow 0$ or $T \rightarrow 0$ both the white noise and the thermal channel reproduce the lossy channel. The common trait among these three noise models is the fact that they can be parametrized as

$$\bar{N}_j = \bar{N} v(\omega_j/\bar{\omega}), \quad (5)$$

where \bar{N} describes a characteristic number of photons in the transmission and $\bar{\omega}$ describes (through an appropriate function v) an eventual characteristic frequency of the channel. The parametrization (5) will be useful in deriving some scaling properties that simplify the derivation. A final noise model we will analyze is a non-linear noise mechanism where the average photon number of the reservoir \bar{N}_j is a function of the average photon number in the message. This type of model is well suited to describe situations in which the noise is due to the action

of some active third party (e.g. an eavesdropper) who is tampering with the transmission. In particular we will analyze a sort of dephasing channel where the average photon number in each transmission mode is preserved, even though some phase correlation is lost. Because of the non-linearity of this noise, the parametrization (5) does not apply to the dephasing channel, but most of the general formalism developed for the other models can still be used in this case.

II. CAPACITIES

In this section we introduce the three different channel capacities that will be analyzed in the paper.

Entanglement assisted capacity.— The one channel capacity that is known to be additive [4, 5] even in the presence of noise is the entanglement assisted capacity C_E . It is defined as the number of bits that can be reliably transmitted per channel use in the presence of an unlimited quantity of prior entanglement shared among the sender and the receiver. This quantity gives a simple upper bound to all the other channel capacities and is conjectured to provide an equivalence class for channels [5]. Analogously, one can define the entanglement assisted quantum capacity Q_E that measures the number of *qubits* that can be reliably transmitted per channel use in the presence of an unlimited quantity of prior entanglement. Using teleportation and superdense coding, it is easy to show that $Q_E = C_E/2$, so that only one of these two quantities needs to be determined [4].

Taking advantage of its additivity property, the entanglement assisted capacity of a multimode channel can be calculated as [5, 6, 7]

$$C_E = \max_{\varrho_j \in \mathcal{H}_j} \left\{ \sum_i I(\mathcal{N}_i, \varrho_i) \right\}, \quad (6)$$

where \mathcal{H}_j is the Hilbert space of the j th mode in the channel and $I(\mathcal{N}_j, \varrho_j)$ is the quantum mutual information defined as [8]

$$I(\mathcal{N}_j, \varrho_j) \equiv S(\varrho_j) + S(\mathcal{N}_j[\varrho_j]) - S((\mathcal{N}_j \otimes \mathbb{1})[\Phi_{\varrho_j}]), \quad (7)$$

(with $S(\varrho_j) = -\text{Tr}[\varrho_j \log_2 \varrho_j]$ the Von Neumann entropy and Φ_{ϱ_j} a purification of the mode input density matrix ϱ_j). The maximization (6) will be performed only using the states ϱ_j that satisfy the average energy constraint

$$\sum_i \hbar\omega_i N_i = \mathcal{E}, \quad (8)$$

where ω_j is the frequency of the j th mode and $N_j = \text{Tr}[a_j^\dagger a_j \varrho_j]$ is its average number of photons. This constraint is fundamental: without any restriction the bosonic channel would have infinite capacity since the Hilbert space that the sender could use for encoding would be infinite-dimensional. The energy constraint introduces an effective cut-off in the dimension of the cod-

ing space [2]. This, of course, mirrors any realistic situation in which the energy available for the transmission is always finite.

Since we are dealing with a Gaussian channel \mathcal{N} we can apply the Holevo-Werner theorem [9] which states that $I(\mathcal{N}_j, \varrho_j)$ reaches its maximum over Gaussian inputs. Moreover, for the noise models we analyze, squeezing the input to the j th mode does not increase its quantum mutual information if the energy of the mode is fixed (see App. A for details). Hence, the maximum value of $I(\mathcal{N}_j, \varrho_j)$ is given by an expression $c_E(N_j, \bar{N}_j, \eta_j)$ that depends only on the number of photons N_j , on the noise parameter \bar{N}_j , and on the quantum efficiency η_j . The explicit form of c_E is evaluated in App. A and is

$$c_E(N_j, \bar{N}_j, \eta_j) = g(N_j) + g(N'_j) - g\left(\frac{D_j + N_j - N'_j - 1}{2}\right) - g\left(\frac{D_j - N_j + N'_j - 1}{2}\right), \quad (9)$$

where

$$N'_j \equiv \eta_j N_j + (1 - \eta_j) \bar{N}_j. \quad (10)$$

is the average photon number in the j th mode at the channel output and

$$D_j \equiv \sqrt{(N_j + N'_j + 1)^2 - 4\eta_j N_j (N_j + 1)}, \quad (11)$$

$$g(x) \equiv \begin{cases} (x+1) \log_2(x+1) - x \log_2(x) & \text{for } x \neq 0 \\ 0 & \text{for } x = 0. \end{cases} \quad (12)$$

In terms of c_E , Eq. (6) becomes

$$C_E = \max_{N_j} \left\{ \sum_i c_E(N_i, \bar{N}_i, \eta_i) \right\}, \quad (13)$$

where the maximization must be performed on the N_j 's that satisfy (8). In Sec. II A we will calculate explicitly the right hand side of (13). First, however, it is convenient to introduce the other channel capacities in order to underline some common features.

Classical capacity.— The classical capacity C measures the quantity of bits that can be sent reliably through the channel per channel use (without assistance of prior entanglement). For the noiseless broadband bosonic channel ($\eta_j = 1$) it has been shown [1, 2] that, under the energy constraint (8),

$$C = \max_{\varrho \in \mathcal{H}} \{S[\varrho]\} = \mathcal{T} R_C, \quad (14)$$

where \mathcal{T} is the transmission time, $\mathcal{H} = \otimes_i \mathcal{H}_i$ is the Hilbert space of the multimode channel (\mathcal{H}_j being the space of the j th mode), and

$$R_C = \frac{1}{\ln 2} \sqrt{\frac{\pi \mathcal{P}}{3 \hbar}} \quad (15)$$

is the classical communication rate in terms of the input power $\mathcal{P} = \mathcal{E}/\mathcal{T}$.

In the presence of noise, however, a recipe to calculate C involving only single uses of the channel, as in the case of Eqs. (6) and (14), is not known. It could be that entangling successive uses of the channel the amount of information transmitted is increased [10, 11]. This would require to consider input states in the Hilbert space $\mathcal{H}^{\otimes n}$ pertaining to n successive uses of the channel. The estimation of C is, hence, a daunting task. Nevertheless, a simple lower bound for it can be obtained considering unentangled coding procedures, where the sender is not allowed to employ codewords which entangle different channel uses. In the multimode channel, a further simplification consists in considering coding procedures where entanglement among the different signal modes a_j is forbidden. This yields the inequality

$$C \geq \max_{p_j(\mu), \sigma_j(\mu)} \left\{ \sum_i \mathcal{X}_{\mathcal{N}_i}(p_i(\mu), \sigma_i(\mu)) \right\}, \quad (16)$$

where $\varrho_j = \int d\mu p_j(\mu) \sigma_j(\mu)$ describes a message in which the μ th “letter” encoded in the density operator $\sigma_j(\mu) \in \mathcal{H}_j$ has probability density $p_j(\mu)$ to be sent in the j th mode and where

$$\mathcal{X}_{\mathcal{N}_j} \equiv S(\mathcal{N}_j[\varrho_j]) - \int d\mu p_j(\mu) S(\mathcal{N}_j[\sigma_j(\mu)]) \quad (17)$$

is the Holevo information. Unlike the case of C_E discussed in the previous section, it is not known whether the maximum of Eq. (16) can be evaluated working only with Gaussian states. However, adopting this strategy one still obtains a tight lower bound for C [9]. Thus, we evaluate $\mathcal{X}_{\mathcal{N}_j}(p_j(\mu), \sigma_j(\mu))$ for the j th mode using coherent states $\sigma_j(\mu) = |\mu\rangle_j \langle \mu|$ weighted with Gaussian probability distribution $p_j(\mu) = \exp[-|\mu|^2/N_j]/(\pi N_j)$. Selecting this encoding we are assuming that, as in the case of C_E , squeezing does not increase the unassisted capacity if there is an average energy constraint on the input state [1, 2, 12, 13]. With this choice, Eq. (16) can be written in a form analogous to (13), i.e.

$$C \geq \max_{N_j} \left\{ \sum_i k(N_i, \bar{N}_i, \eta_i) \right\}. \quad (18)$$

where the maximum must again be taken under the average energy constraint (8). The function k is calculated in App. A and is given by

$$k(N_j, \bar{N}_j, \eta_j) = g(N'_j) - g((1 - \eta_j) \bar{N}_j), \quad (19)$$

with N'_j defined in Eq. (10).

Equation (18) establishes a lower bound for the classical capacity C . Simple upper bounds for C are given by the entanglement assisted capacity C_E of Eq. (33) and by the noiseless classical capacity $\mathcal{T} R_C$ of Eq. (14).

Quantum capacity.— The quantum capacity Q of a channel is the number of qubits that can be sent reliably through the channel per channel use. For the noiseless case one can show that $Q = C$, i.e. for bosonic channel with $\eta_j = 1$ one can show that $Q = \mathcal{T} R_C$. As for the

classical capacity, an expression involving only single uses of the channel is not known for noisy channels: again it could be that the entanglement of successive channel uses might increase Q [14, 15]. Also here we will consider the lower bound obtained by excluding all the coding procedures that make use of entanglement among successive uses of the channel or among different modes. This provides the inequality

$$Q \geq \max_{\varrho_j} \left\{ \sum_i J(\mathcal{N}_i, \varrho_i) \right\}, \quad (20)$$

where

$$J(\mathcal{N}, \varrho) \equiv I(\mathcal{N}, \varrho) - S(\varrho) \quad (21)$$

is the coherent information [14, 16]. Equation (20) is a consequence of the fact that random quantum codes can convey a number of qubits equal to the coherent information of the channel (if it is greater than zero) [14]— for the particular case of the Gaussian channels this same result was proved also in [17]. In evaluating the right side of Eq. (20), we will employ Gaussian states: here the Holevo-Werner theorem does not apply and this choice will further lower the bound (20) on Q . Moreover, we will restrict the analysis to non-squeezed inputs. These considerations allow us to write Eq. (20) as (see App. A)

$$Q \geq \max_{N_j} \sum_i q(N_i, \bar{N}_i, \eta_i), \quad (22)$$

where the maximization must be performed under the energy constraint (8) and (see App. A)

$$q(N_j, \bar{N}_j, \eta_j) = g(N'_j) - g\left(\frac{D_j + N_j - N'_j - 1}{2}\right) - g\left(\frac{D_j - N_j + N'_j - 1}{2}\right), \quad (23)$$

with N'_j and D_j defined in (10) and (11) respectively.

An alternative lower bound for the quantum capacity Q can be obtained by observing that the definitions of C_E in (6) and of I in (7) imply

$$C_E = \max_{\varrho \in \mathcal{H}} \left\{ J(\mathcal{N}, \varrho) + S(\varrho) \right\} \leq \max_{\varrho \in \mathcal{H}} \left\{ J(\mathcal{N}, \varrho) \right\} + \max_{\varrho \in \mathcal{H}} \left\{ S(\varrho) \right\} \leq Q + \max_{\varrho \in \mathcal{H}} \left\{ S(\varrho) \right\}, \quad (24)$$

which for the broadband channel gives $Q \geq C_E - \mathcal{T} R_C$ by employing Eq. (14).

Equations (22) and (24) give two lower bounds to Q . A simple upper bound is given by the entanglement assisted quantum capacity $Q_E = C_E/2$.

A. Lagrange multiplier procedure

In order to determine the values of C_E and the lower bounds for C and Q given by Eqs. (13), (18) and (22),

one needs to perform maximizations of the form

$$W = \max_{N_j} \left\{ \sum_j w(N_j, \bar{N}_j, \eta_j) \right\}, \quad (25)$$

under the constraint given by Eq. (8). In Eq. (25), the quantity W represents C_E or the lower bounds for C or Q depending on whether w is equal to c_E , k or q respectively. The Lagrange multiplier procedure is well suited to perform these constrained maximizations. It amounts to finding the values of $\{N_j\}$ which solve the equations

$$\frac{\partial}{\partial N_j} \left[\sum_i w(N_i, \bar{N}_i, \eta_i) - \frac{1}{\Omega \ln 2} \sum_i \omega_i N_i \right] = 0, \quad (26)$$

where $1/(\Omega \ln 2)$ is the Lagrange multiplier that must be chosen to satisfy the constraint (8) after having solved Eq. (26). The explicit expressions of Eq. (26) for the three capacities are reported in table II. These equations are in general difficult to solve. A first useful simplification is to assume that all the modes have the same quantum efficiency, i.e. $\eta_j = \eta$ for all j . Even though this is a strong assumption, it is still a good description for broadband channels that have a wide spectral transmission window. Under this approximation, it is easy to verify that Eq. (26) has solution that depends on the mode frequency ω_j and on the noise parameters $\bar{\omega}$ and \bar{N} of Eq. (5) as

$$N_j = \mathcal{F}\left(\frac{\omega_j}{\Omega}, \frac{\bar{\omega}}{\Omega}, \bar{N}, \eta\right). \quad (27)$$

To calculate Ω , the energy constraint (8) can be written as

$$\begin{aligned} \frac{\mathcal{E}}{\hbar} &= \sum_i \omega_i \mathcal{F}\left(\frac{\omega_i}{\Omega}, \frac{\bar{\omega}}{\Omega}, \bar{N}, \eta\right) \\ &\simeq \int_0^\infty \frac{d\omega}{\delta\omega} \omega \mathcal{F}\left(\frac{\omega}{\Omega}, \frac{\bar{\omega}}{\Omega}, \bar{N}, \eta\right) \\ &= \frac{\Omega^2}{\delta\omega} \int_0^\infty dx x \mathcal{F}\left(x, \frac{\bar{\omega}}{\Omega}, \bar{N}, \eta\right), \end{aligned} \quad (28)$$

where the sum over the mode index i is approximated with an integral over the mode frequencies, under the assumption of small minimum frequency interval $\delta\omega$ of the channel. This last quantity determines the minimum time $\mathcal{T} = 2\pi/\delta\omega$ needed to transmit a signal in the channel. In order to solve (28) in terms of Ω , it is useful to introduce the adimensional parameter $y_0 = \bar{\omega}/\Omega$. Thus we find

$$\Omega = \left[\frac{2\pi \mathcal{P}}{\hbar f(y_0, \bar{N}, \eta)} \right]^{1/2}, \quad (29)$$

where $\mathcal{P} = \mathcal{E}/\mathcal{T}$ is the average input power,

$$f(y_0, \bar{N}, \eta) \equiv \int_0^\infty dx x \mathcal{F}(x, y_0, \bar{N}, \eta), \quad (30)$$

C_E	$\left(1 + \frac{1}{N_j'}\right) \left(1 + \frac{1}{N_j'}\right)^{\eta_j} = e^{\omega_j/\Omega} \left(1 + \frac{2}{D_j + N_j - N_j' - 1}\right)^{(A_j+1-\eta_j)/2} \left(1 + \frac{2}{D_j - N_j + N_j' - 1}\right)^{(A_j-1+\eta_j)/2}$
C lower bound	$\left(1 + \frac{1}{\eta_j N_j + (1-\eta_j)\bar{N}_j}\right)^{\eta_j} = e^{\omega_j/\Omega}$
Q lower bound	$\left(1 + \frac{1}{N_j'}\right)^{\eta_j} = e^{\omega_j/\Omega} \left(1 + \frac{2}{D_j + N_j - N_j' - 1}\right)^{(A_j+1-\eta_j)/2} \left(1 + \frac{2}{D_j - N_j + N_j' - 1}\right)^{(A_j-1+\eta_j)/2}$

TABLE II: Lagrange equations deriving from (26) for the different capacities. The functions N_j' and D_j are defined in (10) and (11) respectively and $A_j \equiv [(1-3\eta_j)N_j + (1-\eta_j) + (1+\eta_j)N_j'] / D_j$. Notice that the equation pertaining to C can always be solved analytically.

and y_0 is determined by solving (with respect to y) the equation

$$y^2 = \frac{\hbar\bar{\omega}^2}{2\pi\mathcal{P}} f(y, \bar{N}, \eta). \quad (31)$$

If the noise reservoir does not have a characteristic frequency $\bar{\omega}$ (as in the case of the loss, white noise and dephasing), the derivation simplifies since neither \mathcal{F} nor f depend on the parameter y_0 : Eq. (31) does not apply and Ω is already determined by Eq. (29). However, for the sake of generality, we can include also these last cases in the above formalism by assigning to them $\bar{\omega} = 0$ and $y_0 = 0$.

The value of W is finally obtained using Eqs. (27) and (29) to evaluate the sum (25), i.e.

$$\begin{aligned} W &= \sum_i w \left(\mathcal{F} \left(\frac{\omega_i}{\Omega}, \frac{\bar{\omega}}{\Omega}, \bar{N}, \eta \right), \bar{N}_i, \eta \right) \\ &\simeq \int_0^\infty \frac{d\omega}{\delta\omega} w \left(\mathcal{F} \left(\frac{\omega}{\Omega}, \frac{\bar{\omega}}{\Omega}, \bar{N}, \eta \right), \bar{N} v \left(\frac{\omega}{\bar{\omega}} \right), \eta \right) \\ &= \frac{\Omega}{\delta\omega} \int_0^\infty dx w \left(\mathcal{F} \left(x, y_0, \bar{N}, \eta \right), \bar{N} v \left(\frac{x}{y_0} \right), \eta \right), \end{aligned} \quad (32)$$

where the parametrization (5) was employed. Apart from corrections of order $1/\mathcal{T}$ (coming from the approximation of the mode sum with the frequency integral), Eqs. (29) and (32) imply that

$$W = \mathcal{T} R_C \mathcal{W}(y_0, \bar{N}, \eta), \quad (33)$$

where R_C is the noiseless classical rate of Eq. (15) and

$$\begin{aligned} \mathcal{W}(y_0, \bar{N}, \eta) &\equiv \frac{\ln 2}{\pi} \sqrt{\frac{3}{2 f(y_0, \bar{N}, \eta)}} \\ &\times \int_0^\infty dx w \left(\mathcal{F} \left(x, y_0, \bar{N}, \eta \right), \bar{N} v \left(\frac{x}{y_0} \right), \eta \right). \end{aligned} \quad (34)$$

The quantity \mathcal{W} is a proportionality factor that characterizes the dependence of W on the noise parameters η ,

\bar{N} and $\bar{\omega}$. Even though it is in general difficult, if not impossible, to analytically evaluate the expressions \mathcal{F} and \mathcal{W} , one can still provide numerical solutions for these two quantities as will be shown in the following subsections.

When there is no characteristic frequency $\bar{\omega}$ (as in the cases of loss, white noise and dephasing), then $y_0 = 0$ and Eq. (33) tells us that W depends on the input power \mathcal{P} only through the classical communication rate R_C . This means that, in these cases, the capacities of the channel (or at least their bounds) are proportional to the square root of \mathcal{P} just as the noiseless channel classical capacity of Eq. (14). On the other hand, when a characteristic frequency $\bar{\omega}$ does exist (as in the case of the thermal noise), then W depends on \mathcal{P} also through the parameter y_0 , which, according to Eq. (31) is a non-trivial function of $\bar{\omega}^2/\mathcal{P}$. However, for fixed value of this ratio, the $\sqrt{\mathcal{P}}$ proportionality still applies.

III. LOSSY CHANNEL

The simplest channel is the lossy channel where the reservoir is in the vacuum and $\bar{N} = 0$ [7]. In this case, the Lagrange equation solutions \mathcal{F} of (27) for the three capacities are functions only of ω_j/Ω and η . Thus, Eq. (33) gives

$$C_E = \mathcal{T} R_C \mathcal{C}(\eta), \quad (35)$$

$$C \geq \mathcal{T} R_C \mathcal{K}(\eta), \quad (36)$$

$$Q \geq \mathcal{T} R_C \mathcal{Q}(\eta), \quad (37)$$

where the functions \mathcal{C} , \mathcal{K} and \mathcal{Q} take the place of \mathcal{W} in Eq. (34) by replacing w with c_E , k and q . These functions are plotted in Fig. 1. In all these three cases, the dependence on the input power is given by the $\sqrt{\mathcal{P}}$ term in R_C . The alternative lower bound for Q of Eq. (24) becomes

$$Q \geq \mathcal{T} R_C [\mathcal{C}(\eta) - 1]. \quad (38)$$

Both this bound and the function $\mathcal{Q}(\eta)$ of Eq. (37) are positive only for $\eta > 1/2$. This reflects the fact that for $\eta \leq 1/2$ the quantum capacity Q is null. A simple argument based on the no-cloning theorem [18] is sufficient to prove this, as in the case of the erasure channel [19]. In fact, assume that Q is positive for $\eta < 1/2$, and suppose that a third party collects all the photons lost during the transmission: to him the channel would appear to have a quantum efficiency $(1 - \eta > 1/2)$ greater than the one of the receiver. If $Q > 0$, both he and the receiver would be able to reconstruct the quantum information sent through the channel reliably, thus violating the no-cloning theorem. Interestingly this $\eta = 1/2$ bound for the lossy channel has been observed also in tomographic quantum state reconstruction, where the effect of the loss can be deconvolved from the reconstruction only when the detection efficiency is bigger than $1/2$ [20].

Notice that, while \mathcal{C} and \mathcal{Q} must be computed through numerical methods (a partial analytic characterization of $\mathcal{C}(\eta)$ is provided in [7], where, in particular, it is shown that $\mathcal{C}(1) = 2\mathcal{C}(1/2) = 2$), it is possible to determine analytically the value of \mathcal{K} . In fact, the Lagrange equation for \mathcal{C} (see table II) has solution

$$N_j = \mathcal{F}\left(\frac{\omega_j}{\Omega}, \eta_j\right) = \frac{1/\eta_j}{e^{\omega_j/(\Omega\eta_j)} - 1}. \quad (39)$$

When all the η_j are equal, the value of Ω can be calculated directly through the energy constraint (29) ($y_0 = 0$ since there is no characteristic frequency $\bar{\omega}$). In particular, since the function f of Eq. (30) is

$$f(\eta) = \int_0^\infty dx \frac{x/\eta}{e^{x/\eta} - 1} = \eta \frac{\pi^2}{6}, \quad (40)$$

we have $\Omega = [12\mathcal{P}/(\pi\hbar\eta)]^{1/2}$. To evaluate \mathcal{K} through Eq. (34), we need also the term

$$\begin{aligned} \int_0^\infty dx k(\mathcal{F}(x, \eta), \eta) &= \eta \int_0^\infty dy g\left(\frac{1}{e^y - 1}\right) \\ &= \frac{\pi^2 \eta}{3 \ln 2}. \end{aligned} \quad (41)$$

Replacing (40) and (41) in Eq. (34), we finally find

$$\mathcal{K}(\eta) = \sqrt{\eta}. \quad (42)$$

Notice that, from Eq. (14) it follows that in Eq. (36) the equality must hold for $\eta = 1$ and the results of [1, 2] are reobtained.

IV. WHITE NOISE CHANNEL

As in the case of the lossy channel, also the white noise channel has no characteristic frequency $\bar{\omega}$, in fact all noise modes contain the same average number of photons $\bar{N}_j = \bar{N}$. This means that the solutions \mathcal{F} of the Lagrange

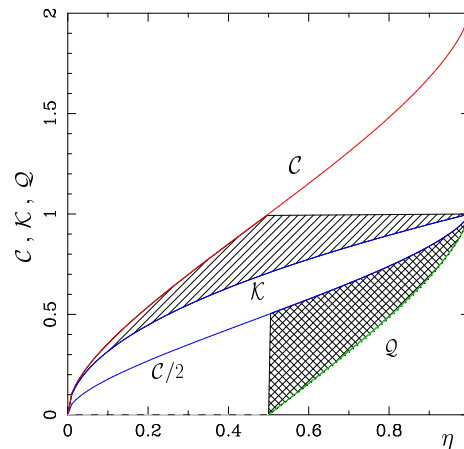


FIG. 1: Plot of the functions $\mathcal{C}(\eta)$, $\mathcal{K}(\eta)$ and $\mathcal{Q}(\eta)$ of Eqs. (35)–(37) for the lossy channel. The function $\mathcal{C}(\eta)$ characterizes the entanglement assisted capacity C_E (upper continuous line). $\mathcal{C}(\eta)$, $\mathcal{K}(\eta)$ and the value 1 (that corresponds to the noiseless classical capacity (14)) bound \mathcal{C} which is restricted to the hatched region. $\mathcal{C}(\eta)/2$ and $\mathcal{Q}(\eta)$ bound the quantum capacity Q which is restricted to the cross-hatched region. The alternative lower bound for Q of Eq. (38) is given by the dotted line, which is almost indistinguishable from $\mathcal{Q}(\eta)$. The quantum capacity Q is null for $\eta < 1/2$ (dashed line). The fact that, for the lossy channel $\mathcal{C}(1) = 2$ is a signature of the superdense coding effect: prior entanglement allows to double the channel capacity [21].

equation are only functions of ω_j/Ω , \bar{N} and η . Thus Eq. (33) gives

$$C_E = \mathcal{T} R_C \mathcal{C}(\bar{N}, \eta), \quad (43)$$

$$C \geq \mathcal{T} R_C \mathcal{K}(\bar{N}, \eta), \quad (44)$$

$$Q \geq \mathcal{T} R_C \mathcal{Q}(\bar{N}, \eta), \quad (45)$$

while Eq. (24) becomes $Q \geq \mathcal{T} R_C [\mathcal{C}(\bar{N}, \eta) - 1]$. As in the previous case, Eqs. (43)–(45) display the square root dependence of the capacities on the input power \mathcal{P} through R_C . The functions \mathcal{C} , \mathcal{K} and \mathcal{Q} for the white noise channel are plotted in Fig. 2 for different values of \bar{N} . Some examples of the numerical solutions $\mathcal{F}(\omega_i/\Omega, \bar{N}, \eta)$ of the Lagrange equations are plotted in Fig. 3.

As for the lossy channel, also here an analytical expression for \mathcal{K} exists. In fact, the Lagrange equation for \mathcal{C} (see table II) has solution

$$N_j = \mathcal{F}\left(\frac{\omega_j}{\Omega}, \bar{N}, \eta_j\right) = \frac{1/\eta_j}{e^{\omega_j/(\eta_j\Omega)} - 1} - \frac{1 - \eta_j}{\eta_j} \bar{N}. \quad (46)$$

Since N_j represents the average photon number in the j th mode, the solution (46) can be used only when $N_j \geq 0$. This condition is satisfied only if the frequency of the mode ω_j is lower than the cut-off frequency $\omega_{max} = \eta \Omega s$, where

$$s \equiv \ln \left[1 + \frac{1}{(1 - \eta)\bar{N}} \right] \quad (47)$$

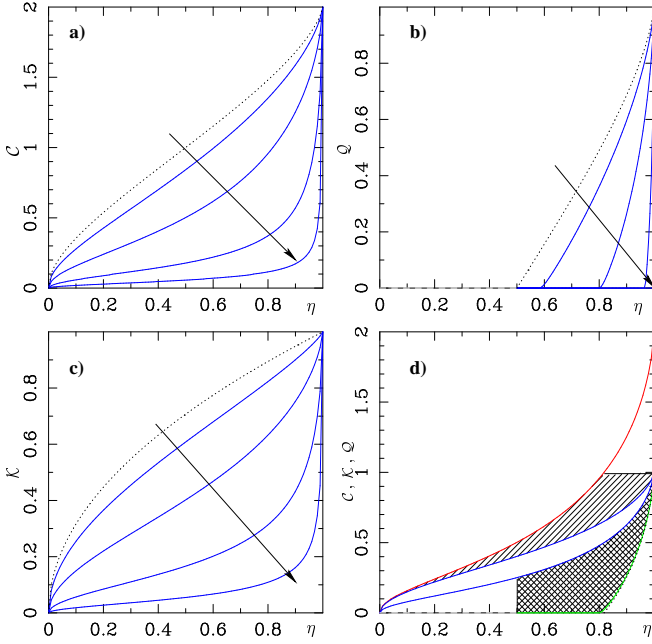


FIG. 2: **a), b), c)** Plot of the functions $\mathcal{C}(\bar{N}, \eta)$, $\mathcal{K}(\bar{N}, \eta)$ and $\mathcal{Q}(\bar{N}, \eta)$ of Eqs. (43)–(45) for the white noise channel with \bar{N} increasing along the direction of the arrows. The dotted lines represents the case $\bar{N} = 0$ from Fig. 1. **d)** Plot of the bounds of the classical (hatched region) and quantum (cross-hatched region) capacities for $\bar{N} = 1$. From top to bottom, the curves are \mathcal{C} , \mathcal{K} , $\mathcal{C}/2$, \mathcal{Q} and the alternative lower bound $\mathcal{C} - 1$, which in this case is practically coincident with \mathcal{Q} .

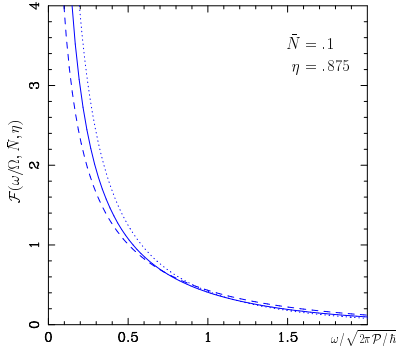


FIG. 3: Examples of the solution $N_j = \mathcal{F}(\omega/\Omega, \bar{N}, \eta)$ of the Lagrange equations for C_E (continuous line), for C (dotted line from Eq. (46)), and for Q (dashed line).

(again we have assumed $\eta_j = \eta$ for all j). For $\omega_j \geq \omega_{max}$, Eq. (46) cannot be used (it gives a negative N_j) so that we assume $N_j = 0$. This physically corresponds to not sending any photons in the high frequency modes: it would be too expensive in energetic terms to contrast the noise in these modes. With this choice, from Eq. (30) we obtain

$$\begin{aligned} f(\bar{N}, \eta) &= \int_0^{\omega_{max}/\Omega} dx x \left[\frac{1/\eta}{e^{x/\eta} - 1} - \frac{1 - \eta \bar{N}}{\eta} \right] \\ &= \eta \left[\Gamma(s) - (1 - \eta) s^2 \bar{N} / 2 \right], \end{aligned} \quad (48)$$

where

$$\Gamma(x) \equiv \int_0^x dy \frac{y}{e^y - 1}. \quad (49)$$

To calculate \mathcal{K} we also need the integral

$$\begin{aligned} & \int_0^\infty dx k(\mathcal{F}(x, \bar{N}, \eta), \bar{N}, \eta) \\ &= \int_0^{\eta s} dx [g(\eta \mathcal{F} + (1 - \eta)\bar{N}) - g((1 - \eta)\bar{N})] \\ &= \eta \left[\int_0^s dx g\left(\frac{1}{e^x - 1}\right) - s g((1 - \eta)\bar{N}) \right]. \end{aligned} \quad (50)$$

Replacing (48) and (50) into Eq. (34) the function $\mathcal{K}(\bar{N}, \eta)$ is determined. Notice that in the limit $\bar{N} \rightarrow 0$, it is possible to show that the function \mathcal{K} converges to $\sqrt{\eta}$ so that one reobtains the results of the lossy channel.

V. THERMAL NOISE

Let us now analyze the case of thermal noise. This noise model does have a characteristic frequency $\bar{\omega} \equiv KT/\hbar$ which depends on the bath temperature T . Since $\bar{\omega} \neq 0$, we need to solve y_0 from Eq. (31) which clearly implies that y_0 is a function of the ratio between the square of the temperature T and the power \mathcal{P} . In this case, $\bar{N} = 1$ and the expressions for the capacities are

$$C_E = \mathcal{T} R_C \mathcal{C}(y_0^{C_E}, \eta), \quad (51)$$

$$C \geq \mathcal{T} R_C \mathcal{K}(y_0^C, \eta), \quad (52)$$

$$Q \geq \mathcal{T} R_C \mathcal{Q}(y_0^Q, \eta), \quad (53)$$

where $y_0^{C_E}$, y_0^C and y_0^Q are the solutions of Eq. (31) for the respective capacities. Moreover, the alternative lower bound of Eq. (24) gives $Q \geq \mathcal{T} R_C [\mathcal{C}(y_0^{C_E}, \eta) - 1]$. The presence of the terms y_0 complicates the dependence of the capacities on the input power \mathcal{P} . However, once the ratio $\hbar(KT)^2/\mathcal{P}$ has been fixed, the usual dependence on the square root of the input power applies. Some numerical plots of \mathcal{C} , \mathcal{K} and \mathcal{Q} are given in Fig. 4 as a function of η and of the temperature T . Some examples of the corresponding Lagrange equation solutions \mathcal{F} are given in Fig. 5.

Again the function \mathcal{K} for the lower bound of the classical capacity can be solved analytically. We will find that below a critical temperature T_c the solutions N_j of the Lagrange equation, i.e.

$$N_j = \mathcal{F}\left(\frac{\omega_j}{\Omega}, \frac{\bar{\omega}}{\Omega}, \eta_j\right) = \frac{1/\eta_j}{e^{\omega_j/(\eta_j \Omega)} - 1} - \frac{(1 - \eta_j)/\eta_j}{e^{\omega_j/\bar{\omega}} - 1} \quad (54)$$

are valid for all frequencies ω_j . On the contrary, when $T > T_c$ a cut-off frequency arises above which (as in the case of the white noise channel) it is convenient not to send photons.

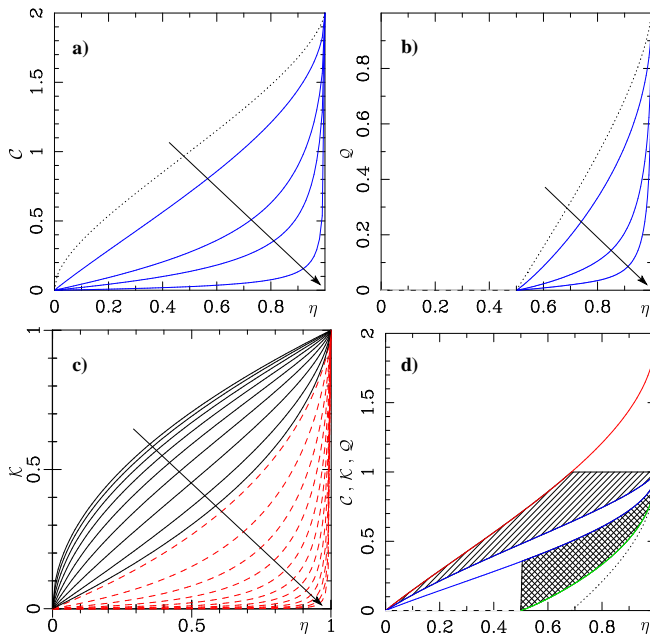


FIG. 4: **a), b), c)** Plot of the functions $\mathcal{C}(y_0^C, \eta)$, $\mathcal{K}(y_0^C, \eta)$ and $\mathcal{Q}(y_0^C, \eta)$ of Eqs. (51)–(53) for the thermal channel with temperature T increasing along the direction of the arrows. The dotted lines represents the case $T = 0$ from Fig. 1. In the plot **c)**, the low temperature regime $T < T_c$ (continuous lines) is obtained from Eq. (57), while the high temperature regime (dashed lines) is obtained from Eq. (60). **d)** Plot of the bounds of the classical (hatched region) and quantum (cross-hatched region) capacities for $R_T/R_C = .41$. From top to bottom, the curves are \mathcal{C} , \mathcal{K} , $\mathcal{C}/2$, \mathcal{Q} and the alternative lower bound $\mathcal{C} - 1$.

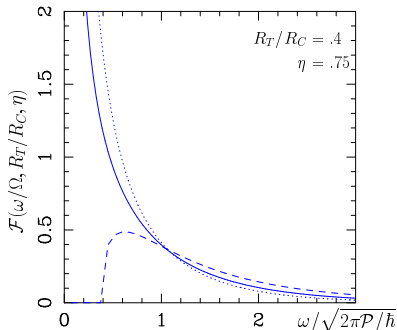


FIG. 5: Examples of the solution $N_j = \mathcal{F}(\omega/\Omega, \bar{N}, \eta)$ of the Lagrange equations for C_E (continuous line), for C (dotted line from Eq. (46)), and for Q (dashed line). It is possible to show that the solutions of the Lagrange equation for Q have two cut-off frequencies for low and high ω . In this graph only the first one is evident.

In the low temperature regime we find

$$y_0^C = \frac{\eta R_T}{[\eta R_C^2 + (1 - \eta)R_T^2]^{1/2}}, \quad (55)$$

where $R_T \equiv \frac{\pi^2}{3 \ln 2} \frac{KT}{h}$, so that the Lagrange multiplier Ω

obtained from the energy constraint (29) is

$$\Omega = \frac{6 \ln 2}{\eta \pi} \sqrt{\eta R_C^2 + (1 - \eta)R_T^2}. \quad (56)$$

Replacing Eqs. (54) and (56) in Eq. (34), we obtain

$$\mathcal{K}(y_0^C, \eta) = \sqrt{\eta + (1 - \eta) \left(\frac{R_T}{R_C}\right)^2} - \frac{\Lambda(1 - \eta) R_T}{\Lambda(1) R_C}, \quad (57)$$

where the dependence on y_0^C derives from (55) and where

$$\Lambda(x) \equiv \ln 2 \int_0^\infty dy g\left(\frac{x}{e^y - 1}\right). \quad (58)$$

Equations (54) and (56) are consistent (i.e. provide a nonnegative N_j for all frequencies) only in the low temperature regime $T \leq T_c \equiv \sqrt{6\mathcal{P}}/(\pi K)$, where $R_C \geq R_T$ and the N_j 's of Eq. (54) are positive quantities for all j . On the other hand, in the high temperature regime ($T > T_c$), the solutions N_j provided by Eq. (54) are valid only for frequencies $\omega_j \leq \omega_{max} \equiv \eta KT(\ln \xi)/(\hbar y_0^C)$, where the parameters y_0^C and ξ are obtained by solving (for $\xi > 1$) the following coupled equations (the first is determined by imposing $N_j = 0$ in Eq. (54), while the second is just Eq. (31)):

$$\xi^{\eta/y_0^C} - (1 - \eta)\xi - \eta = 0 \quad (59)$$

$$\eta \Gamma(\ln \xi) = \left[\frac{1 - \eta}{\eta} \Gamma\left(\frac{\eta \ln \xi}{y_0^C}\right) + \frac{\pi^2}{6} \left(\frac{R_C}{R_T}\right)^2 \right] (y_0^C)^2,$$

with $\Gamma(x)$ defined in Eq. (49). For higher frequencies Eq. (54) gives negative values of N_j and we need to choose $N_j = 0$. With these solutions N_j , one can evaluate y_0^C and Ω through Eqs. (31) and (29) so that from Eq. (34) it is possible to obtain

$$\mathcal{K}(y_0^C, \eta) = \frac{3 \eta \ln 2 R_T}{\pi^2 y_0^C R_C} \times \int_0^{\ln \xi} dx \left[g\left(\frac{1}{e^x - 1}\right) - g\left(\frac{1 - \eta}{e^x \eta/y_0^C - 1}\right) \right]. \quad (60)$$

In the limit $T \rightarrow T_c$, we find $y_0^C \rightarrow \eta$ and $\xi \rightarrow \infty$, and Eq. (60) reduces to (57), i.e. the transition between the high temperature regime and the low temperature regime is continuous. On the other hand, for $T = 0$, we find $R_T = 0$, so from Eq. (57) we reobtain the lossy channel result of Eq. (42). The bounds (57) and (60) are plotted in Fig. 4c for different values of T .

VI. DEPHASING CHANNEL

In this section we will focus on a non-linear noise source where the effect of the reservoir depends on the state of the message. In particular, we consider the case in which the average photon number of the noise source \bar{N}_j is the

C_E	$\left(1 + \frac{1}{N_j}\right)^2 = e^{\omega_j/\Omega} \left(1 + \frac{2}{\tilde{D}_j - 1}\right)^{\frac{2(1-\eta_j)(2N_j+1)}{\tilde{D}_j}}$
C lower bound	$\left(1 + \frac{1}{N_j}\right) = e^{\omega_j/\Omega} \left(1 + \frac{1}{(1-\eta_j)N_j}\right)^{1-\eta_j}$
Q lower bound	$\left(1 + \frac{1}{N_j}\right) = e^{\omega_j/\Omega} \left(1 + \frac{2}{\tilde{D}_j - 1}\right)^{\frac{2(1-\eta_j)(2N_j+1)}{\tilde{D}_j}}$

TABLE III: Lagrange equations for the dephasing channel deriving from (26) for the different capacities.

same as the one (N_j) of the message. The average photon number is hence preserved during the transmission. Of course, this does not mean that the channel is immune to noise: in replacing the lost photons with those from the reservoir, some phase correlations are lost. Under these conditions, imposing $\bar{N}_j = N_j$ in (9), (19) and (23), the values of the functions c_E , k and q become

$$c_E(N_j, \eta_j) = 2[g(N_j) - g((\tilde{D}_j - 1)/2)] \quad (61)$$

$$k(N_j, \eta_j) = g(N_j) - g((1 - \eta_j)N_j) \quad (62)$$

$$q(N_j, \eta_j) = g(N_j) - 2g((\tilde{D}_j - 1)/2), \quad (63)$$

with $\tilde{D}_j \equiv \sqrt{1 + 4N_j(N_j + 1)(1 - \eta_j)}$, from which the Lagrange equations of table III derive to replace those of table II. As in the case of the lossy channel the solutions of the Lagrange equations depend only on ω_j/Ω and η . Hence, the same structure as Eqs. (35)–(37) applies, but here the functions \mathcal{C} , \mathcal{K} and \mathcal{Q} are the ones plotted in Fig. 6.

VII. CONCLUSIONS

In this paper we extend previous analysis on the capacities of broadband bosonic channels with input power constraint [1, 2]. In particular, we analyzed the quantum capacities in the presence of different noise sources. Solutions for the entanglement assisted capacity C_E and upper and lower bounds for the classical and quantum capacities C and Q were provided. At least in the case of unit quantum efficiency (i.e. when the channel is noise free), these bounds are tight since they reproduce the noiseless capacities [1, 2]. Moreover, if the channel noise does not have any characteristic frequency (as in the case of the loss, white noise and dephasing), the square root of the input power dependence (that was known for the noiseless case) is reobtained. Even though all the results in the paper were obtained by considering a uniform quantum efficiency for all the channel modes, the

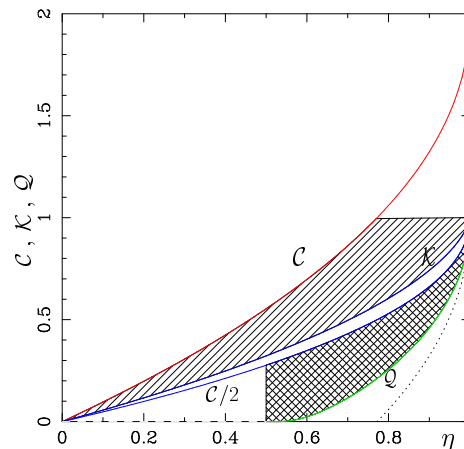


FIG. 6: Plot of the functions $\mathcal{C}(\eta)$, $\mathcal{K}(\eta)$ and $\mathcal{Q}(\eta)$ for the dephasing channel. The hatched region and the cross-hatched region are defined as in Fig. 1 and contain the classical and quantum capacities respectively. The alternative lower bound for Q (i.e. $\mathcal{C}(\eta) - 1$) is given by the dotted line. As for the other channels, it can be shown that Q is null for $\eta < 1/2$ (dashed line).

procedure can be extended also to non uniform configurations. It is also possible to include frequency degerate situations, e.g. where one uses polarization degrees of freedom to encode information. It is still to be determined whether non-linearities in the channel dynamics (where some known interaction couples different modes) can be used [2] to beat the square root dependence, as in the case of the qubit channel discussed in [22].

Acknowledgments

V. G. and L. M. thank Prof. G. M. D’Ariano for useful discussion and comments. This work was funded by the ARDA, NRO, NSF, and by ARO under a MURI program.

APPENDIX A: SINGLE MODE ENTROPIES

In this appendix we calculate some relevant entropic quantities for the single modes when the input is a Gaussian state. We follow the derivation of Holevo and Werner [9] and, for ease of notation, the mode index j is dropped.

Quantum mutual information.— The quantum mutual information $I(\mathcal{N}, \varrho)$ (7) for a single mode can be evaluated just considering the correlation matrix α of the mode input state ϱ , defined as

$$\alpha = \begin{bmatrix} \langle \Delta q^2 \rangle & \frac{1}{2} \langle \{\Delta q, \Delta p\} \rangle \\ \frac{1}{2} \langle \{\Delta p, \Delta q\} \rangle & \langle \Delta p^2 \rangle \end{bmatrix}, \quad (A1)$$

where $\{\cdot, \cdot\}$ denotes the anticommutator, $\Delta q \equiv q - \langle q \rangle$ and $\Delta p \equiv p - \langle p \rangle$, with q and p the two orthogonal

quadratures $q \equiv \sqrt{\hbar/2} (a^\dagger + a)$ and $p \equiv i\sqrt{\hbar/2} (a^\dagger - a)$. In [9] it has been shown that, for a given value of the matrix α , $I(\mathcal{N}, \varrho)$ achieves its maximum value for the Gaussian state

$$\varrho = \frac{\hbar}{2\pi} \int dz \exp \left[-i z \cdot \begin{pmatrix} \Delta q \\ \Delta p \end{pmatrix} - \frac{z \cdot \alpha \cdot z^T}{2} \right], \quad (\text{A2})$$

where z is a real bidimensional line vector. According to Eq. (7), to determine the value of $I(\mathcal{N}, \varrho)$ we need to evaluate the input, output and exchange entropies. Following [9, 13, 23] the input entropy of the Gaussian state ϱ can be calculated as

$$S(\varrho) = g(\sqrt{\lambda_+ \lambda_-} - 1/2), \quad (\text{A3})$$

where the function g is defined in (12) and λ_\pm are the eigenvalues of α/\hbar . In the same way, we can evaluate also the final entropy $S(\mathcal{N}[\varrho])$. In fact, the state $\mathcal{N}[\varrho]$ (evolved by the map \mathcal{N} defined in (1)) is again Gaussian and has correlation matrix

$$\alpha' = \eta \alpha + (1 - \eta) B, \quad (\text{A4})$$

where B is the correlation matrix of the j th noise mode introduced in (3). This means that

$$S(\mathcal{N}[\varrho]) = g(\sqrt{\lambda'_+ \lambda'_-} - 1/2), \quad (\text{A5})$$

where λ'_\pm are the eigenvalues of α'/\hbar . The calculation of the entropy of exchange requires to specify a purification Φ_ϱ of ϱ : a good choice is the two-mode Gaussian state

$$\Phi_\varrho = \left(\frac{\hbar}{2\pi} \right)^2 \int dz \int d\bar{z} \exp \left[-i(\Delta q, \Delta p) \cdot z^T - i(\Delta \bar{q}, \Delta \bar{p}) \cdot \bar{z}^T - (z, \bar{z}) \cdot M \cdot (z, \bar{z})^T / 2 \right], \quad (\text{A6})$$

where the \bar{q} and \bar{p} are quadratures operators acting on an ancillary mode and the 4×4 two-mode correlation matrix M is

$$M = \begin{bmatrix} \alpha & \beta \\ -\beta & \alpha \end{bmatrix}, \quad (\text{A7})$$

with $\beta = \Delta \sqrt{-(\Delta^{-1} \alpha)^2 - \frac{\mathbb{1}}{4}}$, Δ being the 2×2 matrix $\hbar \begin{bmatrix} 0 & 1 \\ -1 & 0 \end{bmatrix}$. The map $\mathcal{N} \otimes \mathbb{1}$ evolves Φ_ϱ into a Gaussian state of the same form of (A6) with correlation matrix

$$M' = \begin{bmatrix} \alpha' & \sqrt{\eta} \beta \\ -\sqrt{\eta} \beta & \alpha' \end{bmatrix}. \quad (\text{A8})$$

According to [9, 13, 23] the entropy of exchange can be calculated as

$$S((\mathcal{N} \otimes \mathbb{1})[\Phi_\varrho]) = \frac{1}{2} \sum_{k=1}^4 g(|\lambda_k| - 1/2), \quad (\text{A9})$$

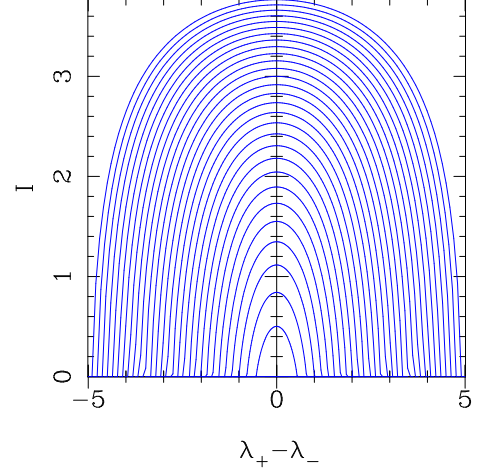


FIG. 7: Plot of the quantum mutual information $I(\mathcal{N}, \varrho)$ of the single mode as a function of $\lambda_+ - \lambda_-$. The different curves correspond to different values of the eigenvalues sum $\lambda_+ + \lambda_-$ increasing from bottom to top. It is evident that the maxima are always achieved for $\lambda_+ = \lambda_-$. The parameters for these plots are $\bar{N} = .1$; $\eta = .8$.

where $\lambda_1, \dots, \lambda_4$ are eigenvalues of the matrix $\Delta_{12}^{-1} M'/\hbar$, Δ_{12} being the 4×4 matrix $\begin{bmatrix} \Delta & 0 \\ 0 & -\Delta \end{bmatrix}$.

In order to evaluate the expressions for the entropies, it is convenient to introduce the following real parametrization:

$$\alpha = \frac{\hbar}{2} \begin{bmatrix} n_0 e^r & c \\ c & n_0 e^{-r} \end{bmatrix}, \quad (\text{A10})$$

where r is the squeezing parameter. These parameters are related through the average number of photons N by the inequalities $\sqrt{c^2 + 1} \leq n_0 = (2N + 1 - m)/\cosh r$ (with $m = \langle q/\hbar \rangle^2 + \langle p/\hbar \rangle^2$): the first relation derives from the Heisenberg uncertainty relation, while the second from the energy constraint. The eigenvalues of α and α' are respectively

$$\lambda_\pm = \frac{1}{2} [n_0 \cosh(r) \pm \sqrt{(n_0 \sinh(r))^2 + c^2}], \quad (\text{A11})$$

$$\lambda'_\pm = \eta \lambda_\pm + (1 - \eta) \hbar (\bar{N} + 1/2), \quad (\text{A12})$$

while the four eigenvalues of the matrix $\Delta_{12}^{-1} M'/\hbar$ are $\lambda_{1,2,3,4} = \pm[(L_0 \pm \sqrt{L_1 + L_0^2})/8]^{1/2}$, where

$$L_0 = -(1 + \eta^2) - 4(1 - \eta)^2 \bar{N}^2 - 4(1 - \eta)[1 - \eta + \eta(\lambda_+ + \lambda_-)]\bar{N} - 2\eta(1 - \eta)(\lambda_+ + \lambda_-) - 4(1 - \eta)^2 \lambda_+ \lambda_- \quad (\text{A13})$$

$$L_1 = -8(1 - \eta)(1 + 2\bar{N})[2(1 - \eta)(1 + 2\bar{N})\lambda_+ \lambda_- + \eta(\lambda_+ + \lambda_-)] - 4\eta^2. \quad (\text{A14})$$

From these equations and from the definition (7) it is evident that the entropies of Eqs. (A3) depend on the parameters n_0 , r and c only through the eigenvalues λ_{\pm} of α . Since these quantities are related with the average number of photons N by

$$\lambda_+ + \lambda_- = 2N + 1 - m, \quad (\text{A15})$$

one can show that the maximum of $I(\mathcal{N}, \varrho)$ for fixed N and m is obtained for $\lambda_+ = \lambda_-$ (see Fig. 7). According to Eq. (A11), this is equivalent to requiring $r = 0$ (no squeezing) and $c = 0$ (maximally mixed states). Imposing $\lambda_+ = \lambda_-$ and maximizing with respect to m in the above relations, one easily finds that the entropies become

$$S(\varrho) = g(N) \quad (\text{A16})$$

$$S(\mathcal{N}[\varrho]) = g(N') \quad (\text{A17})$$

$$S((\mathcal{N} \otimes \mathbb{1})[\Phi_{\varrho}]) = g\left(\frac{D + N - N' - 1}{2}\right) \quad (\text{A18})$$

$$+g\left(\frac{D - N + N' - 1}{2}\right),$$

where N' and D are defined in (10) and (11). From these relations it is immediate to show that the maximum of the quantum mutual information for a given value of the average photon number N is given by Eq. (9).

Coherent information.— Replacing (A16)–(A18) in Eq. (21) allow us to calculate the value of the coherent information $J(\mathcal{N}, \varrho)$ for Gaussian states of Eq. (A2) with no squeezing and $m = 0$. This gives the function q of Eq. (23).

Holevo quantity.— To calculate the Holevo quantity $\chi_{\mathcal{N}}$ for the code introduced in Sec. II we can use the above results. In fact both the global state ϱ and its components $\sigma(\mu)$ are Gaussian states of the form (A2), with correlation matrices $\hbar(N + 1/2)\mathbb{1}$ and $\hbar\mathbb{1}/2$ respectively. Hence it is immediate to calculate the entropies that allow to obtain the value of $\chi_{\mathcal{N}}$ reported in Eq. (19).

-
- [1] J. P. Gordon, in *Advances in Quantum Electronics* edited by J. R. Singer (Columbia University, New York, 1961), p. 509; H. P. Yuen and M. Ozawa, *Phys. Rev. Lett.* **70**, 363 (1992).
- [2] C. M. Caves and P. D. Drummond, *Rev. of Mod. Phys.* **66**, 481 (1994).
- [3] C. H. Bennet and P. W. Shor, *IEEE Trans. Inform. Theory* **44**, 2724 (1998).
- [4] C. H. Bennett, P. W. Shor, J. A. Smolin, and A. V. Thapliyal, *Phys. Rev. Lett.* **83**, 3081 (1999).
- [5] C. H. Bennett, P. W. Shor, J. A. Smolin, and A. V. Thapliyal, *IEEE Trans. Inform. Theory* **48**, 2637 (2002), eprint quant-ph/0106052.
- [6] A. S. Holevo eprint quant-ph/0106075.
- [7] V. Giovannetti, S. Lloyd, L. Maccone, and P. W. Shor, *Phys. Rev. Lett.* accepted for publication, eprint quant-ph/0304020.
- [8] C. Adami, N. J. Cerf, *Phys. Rev. A* **56**, 3470 (1997).
- [9] A. S. Holevo and R. F. Werner, *Phys. Rev. A* **63**, 032312 (2001).
- [10] P. Hausladen, R. Jozsa, B. Schumacher, M. Westmoreland, and W. K. Wootters, *Phys. Rev. A* **54**, 1869 (1996); B. Schumacher and M. D. Westmoreland, *Phys. Rev. A* **56**, 131 (1997).
- [11] A. S. Holevo, *IEEE Trans. Inform. Theory* **44**, 269 (1998).
- [12] M. Sohma and O. Hirota eprint quant-ph/0105042; M. Sohma and O. Hirota, *Phys. Rev. A* **65**, 022319 (2002).
- [13] A. S. Holevo, M. Sohma, and O. Hirota, *Phys. Rev. A* **59**, 1820 (1999).
- [14] S. Lloyd, *Phys. Rev. A* **55**, 1613 (1997).
- [15] H. Barnum, M. A. Nielsen, and B. Schumacher, *Phys. Rev. A* **57**, 4153 (1998); H. Barnum, J. A. Smolin, and B. M. Terhal, *Phys. Rev. A* **58**, 3496 (1998).
- [16] B. Schumacher and M. A. Nielsen, *Phys. Rev. A* **54**, 2629 (1996).
- [17] J. Harrington and J. Preskill, *Phys. Rev. A* **64**, 062301 (2001).
- [18] W. K. Wootters and W. H. Zurek, *Nature* **299**, 802 (1982).
- [19] C. H. Bennett, D. P. DiVincenzo and J. A. Smolin, *Phys. Rev. Lett.* **78**, 3217 (1997).
- [20] G. M. D'Ariano, U. Leonhardt, and H. Paul, *Phys. Rev. A* **52**, R1801 (1995).
- [21] C. H. Bennett and S. J. Wiesner, *Phys. Rev. Lett.* **69**, 2881 (1992).
- [22] S. Lloyd, *Phys. Rev. Lett.* **90**, 167902 (2003).
- [23] A. S. Holevo in *Proceedings of the 4th International Conference on Quantum Communication, Measurement and Computing, Evanston* (1998), eprint quant-ph/9809022.